Instantaneous power variance and radio frequency to dc conversion efficiency of wireless power transfer systems

Citation for published version:
Blanco, J, Bolos, F & Georgiadis, A 2016, 'Instantaneous power variance and radio frequency to dc conversion efficiency of wireless power transfer systems', *IET Microwaves, Antennas and Propagation*, vol. 10, no. 10, pp. 1065-1070. https://doi.org/10.1049/iet-map.2015.0790

Digital Object Identifier (DOI):
10.1049/iet-map.2015.0790

Link:
Link to publication record in Heriot-Watt Research Portal

Document Version:
Peer reviewed version

Published In:
IET Microwaves, Antennas and Propagation

Submission for IET MAP Journal

Instantaneous Power Variance (IPV) and RF-dc Conversion Efficiency of Wireless Power Transfer Systems

Javier BLANCO[1], Ferran BOLOS[1], Apostolos GEORGIADIS[1*]

[1]Centre Tecnologic de Telecomunicacions de Catalunya (CTTC), Department of Microwave Systems and Nanotechnology, Avda Carl Friedrich Gauss 7, 08860 Castelldefels, Spain
[*]apostolos.georgiadis@ieee.org

Abstract: This paper compares the maximum rectifier RF-dc conversion efficiency for various input signals with random modulation. The instantaneous power variance (IPV) is proposed as an easy to compute parameter to classify the effect of modulation on the obtained rectifier efficiency. A prototype UHF rectifier is used to simulate as well as measure the performance of randomly modulated signals with BPSK, QPSK, 8PSK and 64QAM modulation. In addition to considering different modulation formats, the roll-off factor of the baseband filter is also varied due to the fact that it has a strong impact on the time-varying nature of the signal envelope. For the given rectifier, it is shown that the peak RF-dc conversion efficiency versus the output load is shifter to larger load values for signals with higher IPV. Furthermore, by comparing signals with different time-varying envelope characteristics it is shown that IPV represents a more accurate signal characteristic than peak-to-average-power-ration (PAPR) in terms of properly characterising the effect of modulation on the rectifier efficiency.

1. Introduction

RF Energy harvesting and wireless power transfer are important technologies which permit pure battery-less operation or alternatively significantly extending the battery lifetime and the energy autonomy of sensor, identification and communication circuits. The potential of the technologies has spurred a strong interest in terms of applications related to radio frequency identification (RFID), the Internet-of-Things (IoT), biomedical and others [1][2][3][4][5][6][7][8]. Recently, the use of signals with a time-varying envelope, such as multi-sines [9][10][11], chaotic [12], white noise [13] or randomly modulated signals [13][14] in wireless power transfer or energy harvesting applications has been investigated due to the fact that under certain input power and output load conditions, such signals can provide a higher RF-dc conversion efficiency than traditionally used continuous wave (CW) signals.

The peak-to-average-power-ratio (PAPR) measure has been used to classify the performance of signals with time-varying envelope [9][10][11][13]. Due to its simplicity, PAPR captures the essential effect of a time varying envelope which results in instantaneous peak power levels which can be much higher than the average signal power, and they can lead to larger mixing products at dc and consequently to a higher RF-dc efficiency when the input signal average power is low and does not bias the nonlinear rectifier element at an operating point which produces significant dc mixing products.

In this paper, instead of PAPR, we propose the use of instantaneous power variance (IPV) to characterize the effect of the time-varying envelope on the obtained RF-dc conversion efficiency. While PAPR reveals the presence of peaks in the signal, IPV presents a more accurate measure to quantify the frequency of occurrence of such peaks which can have a profound effect on the RF-dc conversion efficiency of rectifier circuits. IPV can be easily computed in simulation or measurements from the complementary cumulative distribution function (CCDF) of the signal.

The paper is structured as follows. Section 2 presents the theoretical analysis including the definition of IPV and the simulation and measurement setups which have been used to evaluate IPV and PAPR. Section 3 describes the measurement setup which was used to compare the different input signals with respect to the obtained RF-dc rectifier efficiency. Section 4, shows measurements of different modulated signals applied to UHF rectifier circuit and evaluation of the obtained RF-dc conversion efficiency for different output loads and input power levels. Finally, the conclusions of this work are presented.

2. Theoretical analysis and time-varying signal characterization

The various signals having a time-varying envelope used in this paper are compared based on their instantaneous power variance (IPV) σ_P^2 defined as

$$\sigma_P^2 = E[(P - P_A)^2] \tag{1}$$

where $E[\ ]$ denotes expectation, $P = P(t)$ the instantaneous power and $P_A = E[P]$ the average power. IPV by definition can be computed once the probability density function (pdf) $f_p(p)$ of the instantaneous power is known, or alternatively using the cumulative distribution (CDF) $F_p(p) = \Pr\{P < p\} = \int_{-\infty}^{p} f_p(p)dp$ or complementary cumulative distribution (CCDF) $\bar{F}_p(p) = \Pr\{P > p\} = 1 - F_p(p)$ [15] as

$$\sigma_P^2 = \int (P - P_A)^2 f_p(p)dp = \int (P - P_A)^2 dF_p = -\int (P - P_A)^2 d\bar{F}_p \tag{2}$$

where the average power P_A is computed as

$$P_A = \int P f_p(p)dp = \int P dF_p = -\int P d\bar{F}_p \tag{3}$$

The integrals of the continuous instantaneous power random variable p integrate the sample space of p.

This article has been accepted for publication in a future issue of this journal, but has not been fully edited.
Content may change prior to final publication in an issue of the journal. To cite the paper please use the doi provided on the Digital Library page.

Randomly modulated signals with BPSK, QPSK, 8PSK and 64QAM modulation were generated in Keysight Ptolemy simulator. The setup included a random bit generator based on a pseudorandom generator with a linear feedback shift register of length 23 cells, followed by mapping of the bit sequence to complex symbols based on the desired modulation format. The complex symbols are then separated to two real I and Q symbol sequences which are filtered with a square root raised cosine (RRC) FIR filter with roll-off factor β ($0 < \beta < 1$). The RRC filter is a finite impulse response (FIR) filter with impulse response length of 61 samples which interpolates the symbol sequence to 8 samples per symbol. Following the RRC filter, the real I and Q sequences are combined into a complex sample sequence. The complex sequence represents the modulated signal envelope which is sampled at 1/8 of the symbol rate of 500 ksps and up-converted to a carrier frequency of 915 MHz. Ptolemy is then used to compute the PAPR and the CCDF function of each signal for different modulation formats and values of the RRC filter roll-off factor β for a given P_A. The functional blocks of the simulation setup are shown in Fig. 1a. A measurement test-bench was also created [16] using a digital signal generator, spectrum analyser and vector signal analyser (VSA) software shown in Fig. 1b.

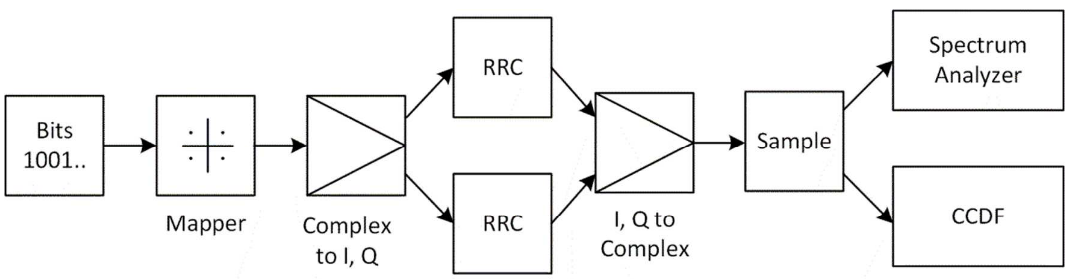

a)

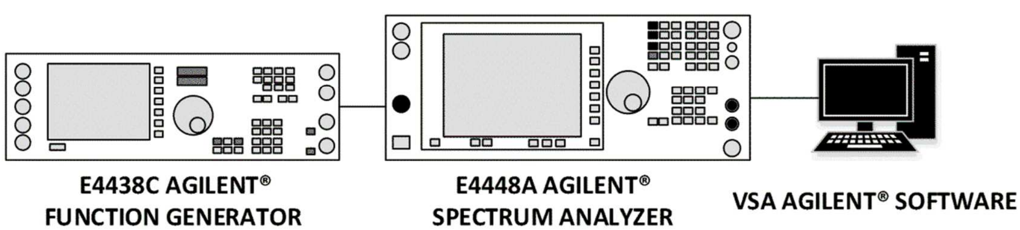

b)

Fig. 1. Simulation setup based on Keysight Ptolemy a) measurement test-bench b) used to evaluate the instantaneous power variance of different randomly modulated signals.

The simulated and measured PAPR of various modulated signals is shown in Fig. 2.

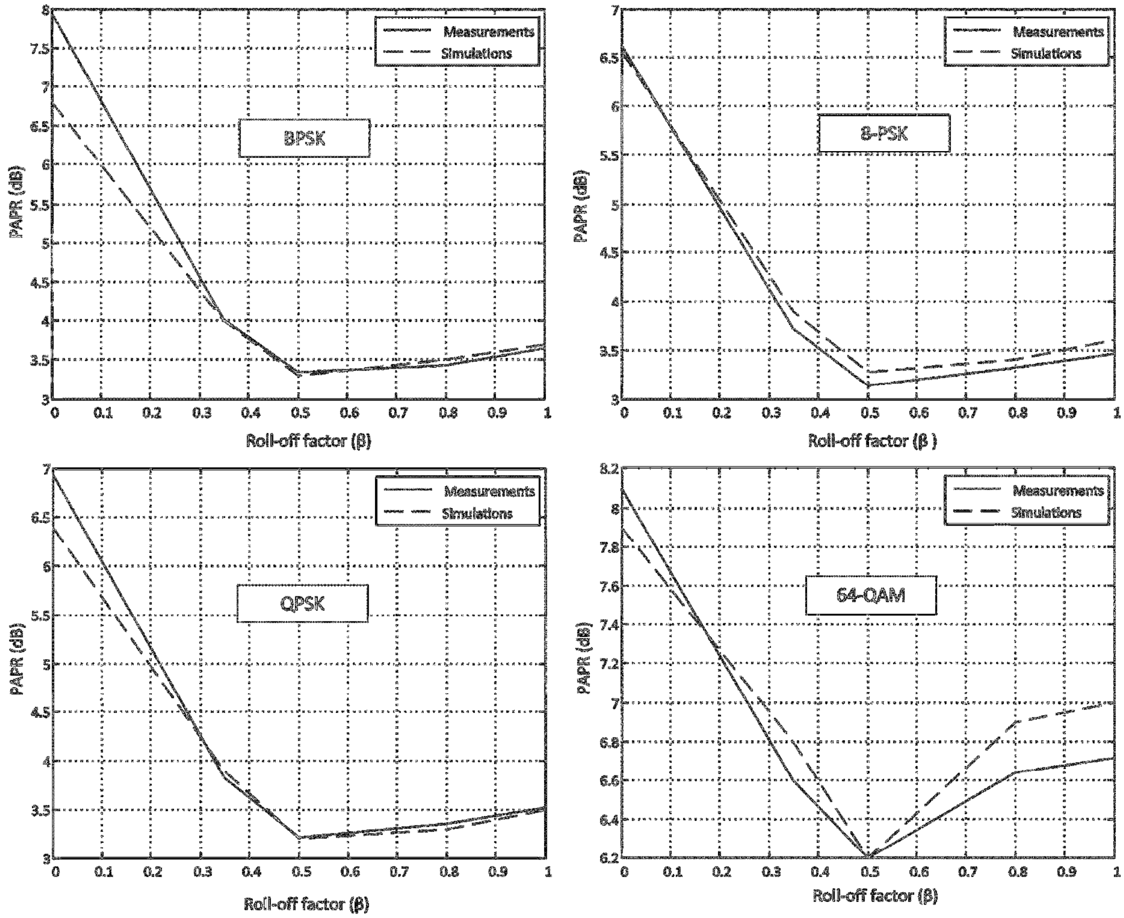

Fig. 2. Simulated and measured PAPR of different modulated signals for different roll-off factor values. The average power is -20 dBm and the symbol rate 500 ksps.

It is seen that there is good agreement between measurement and simulation. The IPV can be computed from the signal CCDF curve by integration using (2). The VSA software provides the measured CCDF in real time, however it only gives the CCDF values for instantaneous power values higher than the average power. As a result it was not possible to compute the instantaneous power variance from the measured CCDF values provided by the VSA. An example is shown in Fig. 3 which compares the simulated and measured CCDF curves for a BPSK signal with roll-off factor $\beta = 1$. Due to the obtained good agreement between simulation and measurement for the available instantaneous power values through the measurements, the simulated CCDF curve was used to compute the IPV for the modulation formats and roll-off factor values of Fig. 2 and it is shown in Fig. 4.

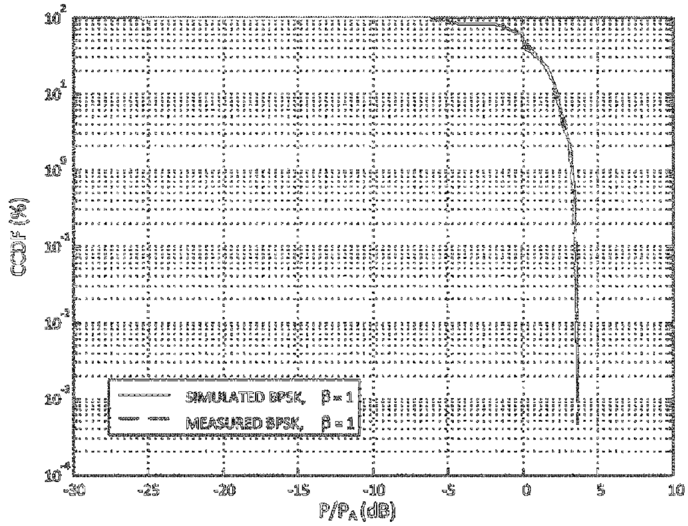

Fig. 3. CCDF curve of a BPSK signal with roll-off factor $\beta = 1$ obtained from simulation and measurement. The abscissa corresponds to instantaneous power over average power ratio measured in dB.

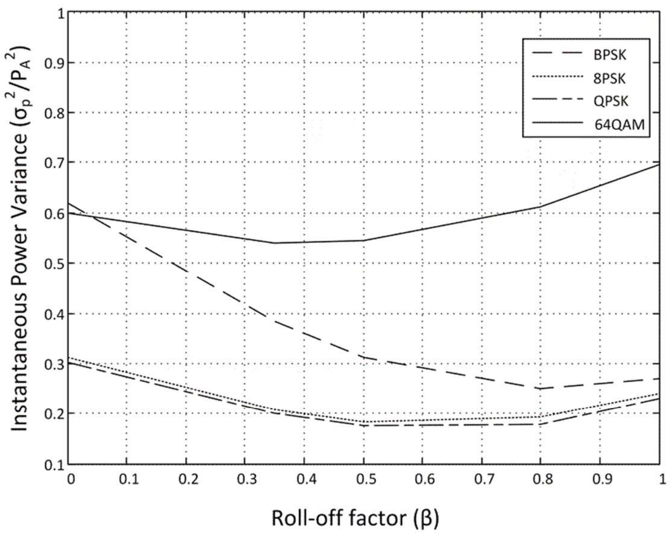

Fig. 4. Simulated IPV of different modulated signals for different roll-off factor values. The average power is -20 dBm and the symbol rate 500 ksps. The IPV is normalized as ${\sigma_p}^2/P_A^2$.

3. RF-dc conversion efficiency measurement setup

A UHF series diode rectifier was used to evaluate the efficiency of the various modulated signals, shown in Fig. 5a. The rectifier is based on a series connected Skyworks SMS7630 Schottky diode (D) and was also used in [16]. A quarter wavelength long shorted stub at 915 MHz is used at the input of the diode in order to provide a short at dc and at the second harmonic frequency (1830 MHz). A T-type matching network formed by two off-the-shelf series inductors and a shunt capacitor is used to match the impedance

This article has been accepted for publication in a future issue of this journal, but has not been fully edited.
Content may change prior to final publication in an issue of the journal. To cite the paper please use the doi provided on the Digital Library page.

of the rectifier to the source 50 Ohm impedance at 915 MHz. The values of the inductors are L_1 = 3.3 nH and L_2 = 43 nH (both from Coilcraft) and the value of the capacitor is C_1 = 3 pF (from Murata). At the output of the rectifier a combination of a C_L = 10 nF shunt capacitor from Murata and a 20 kΩ trimmer variable resistor used as the rectifier load R_L, form a low pass filter which only allows the dc component of the signal. A prototype circuit was built on a 20 mil thick Arlon A25N substrate with dielectric permittivity of 3.38 and loss tangent of 0.0025. A photo of the fabricated prototype can be seen in Fig 5b. The RF-dc efficiency measurement setup [16] consists of a Keysight ESG signal generator used to provide the modulated waveforms, the rectifier circuit and a digital multimeter, shown in Fig. 5c and Fig. 5d.

The RF-dc conversion efficiency is evaluated as

$$\eta_A = \frac{P_{L,dc}}{P_A} \tag{4}$$

where P_A is the available average input power at the input of the rectifier circuit and $P_{L,dc}$ the output dc power on the load R_L.

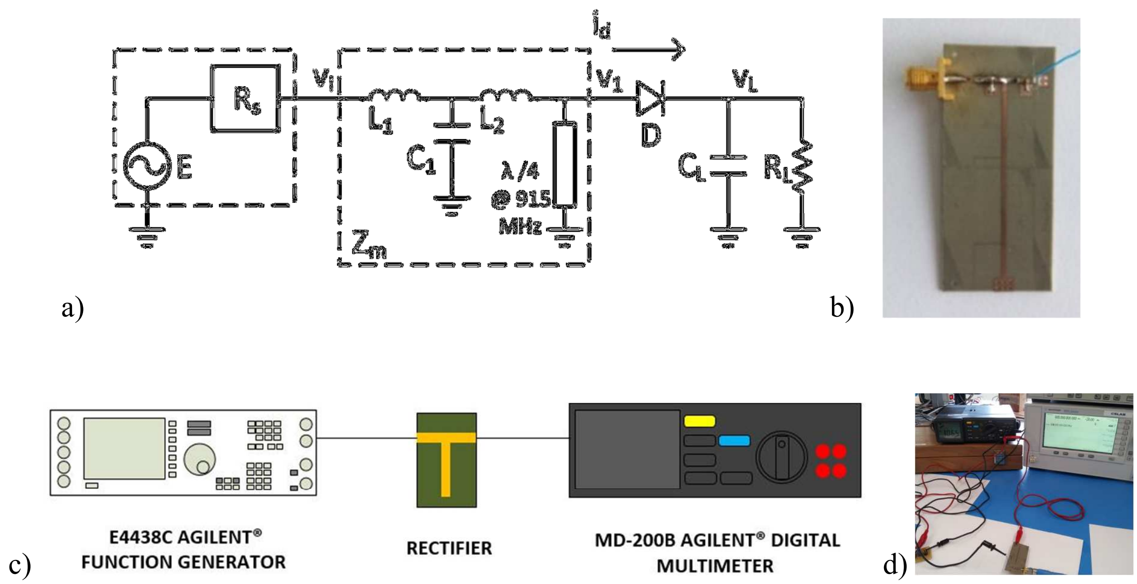

Fig. 5. RF-dc conversion efficiency measurement setup: a) UHF rectifier circuit diagram b) rectifier prototype, c) measurement test-bench block diagram, d) photo of the measurement setup.

This article has been accepted for publication in a future issue of this journal, but has not been fully edited.
Content may change prior to final publication in an issue of the journal. To cite the paper please use the doi provided on the Digital Library page.

4. RF-dc efficiency measurements

The measured RF-dc efficiency corresponding to different modulated signals is shown in Fig. 6, for two average input power levels of -20 dBm and 0 dBm and for different output load values.

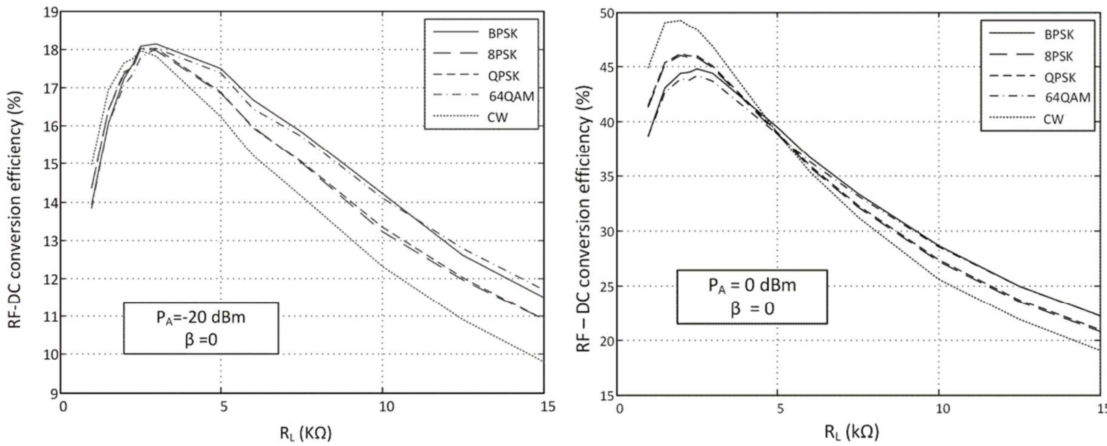

Fig. 6. RF-dc conversion efficiency measurements [16].

Using the PAPR and IPV results of Fig. 2 and Fig. 4 respectively, one can see from the efficiency measurements of Fig. 6 that signals with higher PAPR and IPV values tend to lead to higher RF-dc conversion efficiencies at larger load values [16]. This is the result of the fact that the load corresponding to the peak efficiency appears to shift to larger values as the PAPR and IPV increase.

IPV captures in a more accurate manner the instantaneous power behaviour of the modulated signals than PAPR, since it does not simply identify the presence of a peak power value, but it captures in an average manner the presence of multiple peaks as expressed in detail in the CCDF function. As an example one may consider a QPSK signal with roll-off factor 0 and a 64QAM signal with roll-off factor 1, whose measured CCDF curves are shown in Fig. 7.

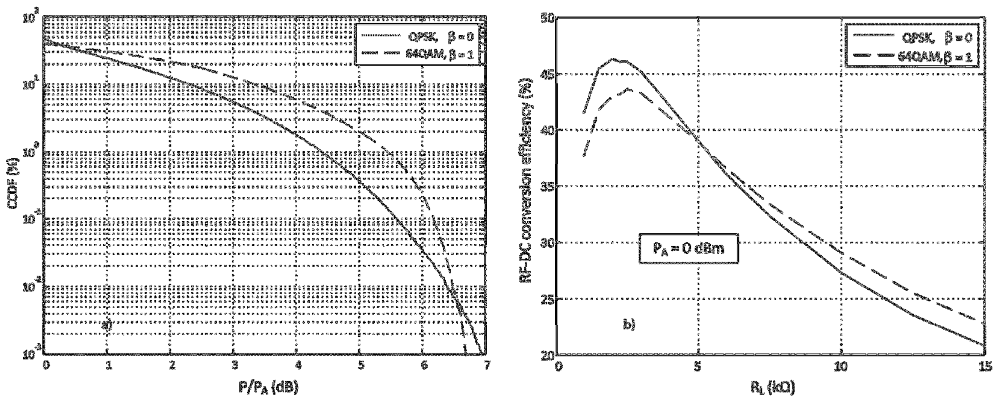

Fig. 7. Comparison of RF-dc conversion efficiency of a QPSK and 64QAM signal with similar PAPR but different IPV characteristics: a) CCDF and b) RF-dc conversion efficiency.

Both signals have the same average power of 0 dBm but the QPSK signal has 7 dB PAPR and the 64QAM signal a slightly lower PAPR of 6.7 dB. However, as can be expected from the CCDF curves the 64QAM signal has a higher IPV of 0.697 compared to QPSK with IPV of 0.302. Note that the IPV values are normalized to the average power as $\sigma_p{}^2/P_A^2$. While the QPSK signal may exhibit a larger peak with a very low probability of occurrence, the 64QAM signal has smaller peaks which however come with a higher probability. As a result the 64QAM signal obtains its maximum efficiency at a larger load value and exhibits higher efficiency at larger load values compared to the QPSK signal.

The same effect can also be seen more clearly when we compare a 4-tone signal with a 64QAM with a roll off factor β = 0.5, shown in Fig. 8. Initially a 4-tone signal was selected consisting of 4 in-phase tones with 1 MHz spacing centered at 915 MHz. The 4-tone signal had a PAPR value of 6.2 dB. In a second step, the roll-off factor of a 64QAM signal was varied until its PAPR was equal to the 6.2 dB value of the 4-tone signal. Both signals have the same average power of 0 dBm. As shown in Fig. 8a, while the PAPR of both signals is the same, their CCDF curves and their IPV values are very different. The 4-tone signal has an IPV of 1.804 while the 64QAM signal has an IPV of 0.545. Consequently, the RF-dc conversion efficiency curves corresponding to the two signals are very different (Fig. 8b). The 4-tone signal with a higher IPV obtains its maximum efficiency at a larger load value and it performs much better than the 64QAM signal in terms of efficiency at higher load values. In order to further appreciate the difference between the two signals their time domain envelope magnitude is simulated and shown in Fig. 9. One can see that in the case of the 4-tone signal there is a greater variation between large peaks and smaller peaks, while in the case of the 64QAM signal the envelope takes values which are more confined within an average value.

5. Conclusion

The RF-dc conversion efficiency of modulated signals was studied by comparing simulation results and measurements on a fabricated UHF prototype rectifier. In the recent literature PAPR has been used to indicate the effect of a time-varying envelope on the rectifier efficiency. In this work, the instantaneous power variance (IPV) is proposed to classify the performance of such signals. IPV is able to describe more accurately than PAPR the variation of the instantaneous power and the occurrence of signal peaks which have a direct effect on the obtained RF-dc conversion efficiency of signals with a time-varying envelope when applied to a rectifier. Two examples of signals with similar PAPR but different IPV and also different performance in terms of the obtained rectifier efficiency are shown to demonstrate that IPV is a more accurate indicator of the effect of the signal characteristics on the rectifier performance. The dependence of the optimal rectifier load on the transmitted signal properties suggests the possibility of tailoring the optimal load and consequently the obtained RF-dc conversion efficiency through a careful design of the transmitted signals. One should further note that ultra-low power circuits such as passive RFID tags which require a few tens of μW power to operate represent examples of high impedance rectifier loads which can potentially take advantage of using signals with high IPV or PAPR for transmission of power.

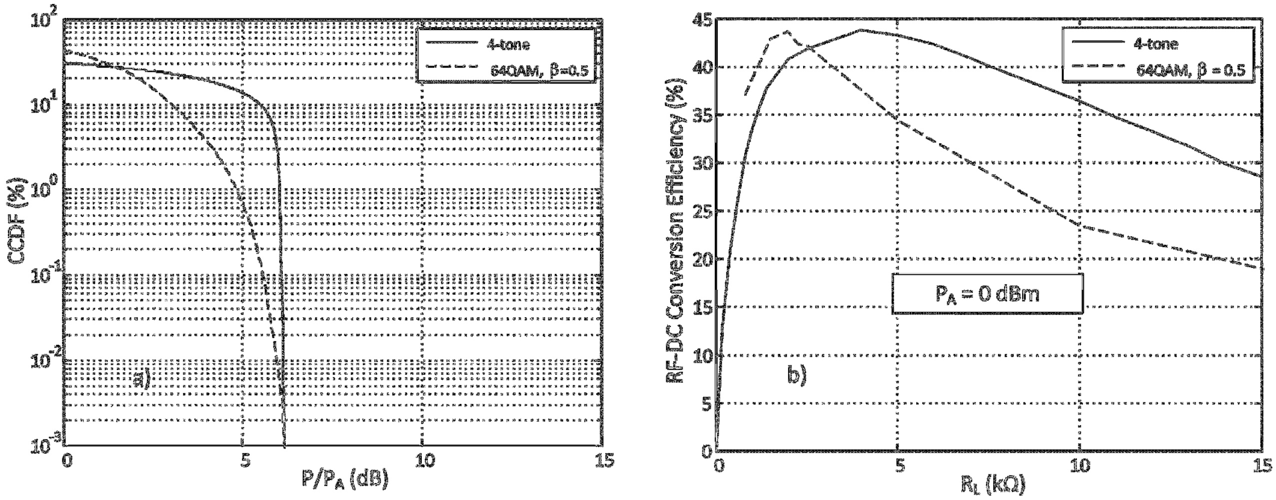

Fig. 8. Comparison of RF-dc conversion efficiency of a 4-tone and 64QAM (β = 0.5) signal with similar PAPR but different IPV characteristics: a) CCDF, b) RF-dc conversion efficiency.

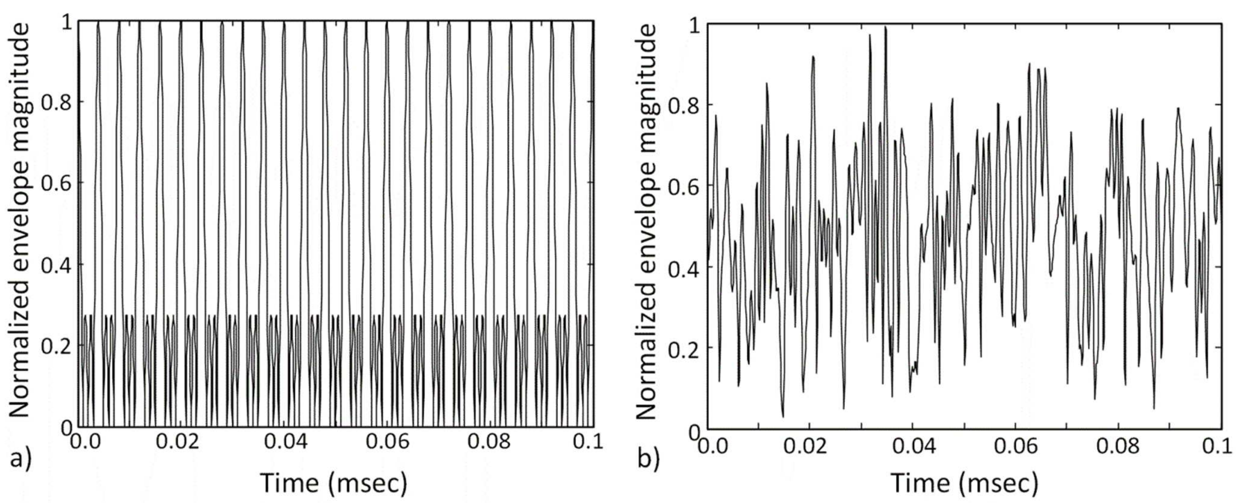

Fig. 9. Simulated time domain envelope of a 4-tone signal with 1 MHz tone spacing and a 64QAM (1 Msps, β = 0.5) signal with the same average power and approximately the same PAPR = 6.2 dB but different IPV characteristics: a) 4-tone, b) 64QAM.

6. Acknowledgments

This work was supported by EU COST Action IC1301 Wireless Power Transmission for Sustainable Electronics and Marie Curie EU H2020 Marie Sklodowska-Curie grant agreement No 661621.

7. References

[1] Kim S., Vyas, R., Bito, *et al.*, "Ambient RF Energy-Harvesting Technologies for Self-Sustainable Standalone Wireless Sensor Platforms," Proceedings of the IEEE, 2014, **106**, (11), pp.1649-1666.

[2] Dolgov, A., Zane, R., Popovic, Z., "Power Management System for Online Low Power RF Energy Harvesting Optimization," IEEE Transactions on Circuits and Systems I: Regular Papers, 2010, **57**, (7), pp. 1802-1811.

[3] Ladan, S., Guntupalli, A.B., Wu, K., "A High-Efficiency 24 GHz Rectenna Development Towards Millimeter-Wave Energy Harvesting and Wireless Power Transmission," IEEE Transactions on Circuits and Systems I: Regular Papers, 2014, **61**, (12), pp. 3358-3366.

[4] Pandey, J., Liao, Y.T., Lingley, A. *et al.*, "A Fully Integrated RF-Powered Contact Lens With a Single Element Display," IEEE Transactions on Biomedical Circuits and Systems, 2010, **4**, (6), pp. 454-460.

[5] Yeager, D.J., Holleman, J., Prasad, R. *et al.*, "NeuralWISP: A Wirelessly Powered Neural Interface With 1-m Range," IEEE Transactions on Biomedical Circuits and Systems, 2009, **3**, (6), pp. 379-387.

[6] Hsieh, P.H., Chou, C.H., Chiang, T., "An RF Energy Harvester With 44.1% PCE at Input Available Power of -12 dBm," IEEE Transactions on Circuits and Systems I: Regular Papers, 2015, **62**, (6), pp. 1528-1537.

[7] Collado, A., Georgiadis, A., "Conformal Hybrid Solar and Electromagnetic (EM) Energy Harvesting Rectenna," IEEE Transactions on Circuits and Systems I: Regular Papers, 2013, **60**, (8), pp. 2225-2234.

[8] Olgun, U., Chen, C.-C., Volakis, J.L., "Design of an efficient ambient WiFi energy harvesting system," in IET Microwaves, Antennas & Propagation , 2012, (6), 11, pp.1200-1206.

[9] Trotter, M.S., Griffin, J.D., Durgin, G.D., "Power-optimized waveforms for improving the range and reliability of RFID systems," Proc. Int. Conf. on RFID, Orlando, USA , 27-28 April 2009, pp. 80-87.

[10] Correia, R., Borges Carvalho, N., Kawasaki, S., "Backscatter radio coverage enhancements using improved WPT signal waveform," Proc 2015 IEEE Wireless Power Transfer Conference (WPTC), Boulder, USA, pp.1-3, 13-15 May 2015.

[11] Boaventura, A., Belo, D., Fernandes, R., *et al.*, "Boosting the Efficiency: Unconventional Waveform Design for Efficient Wireless Power Transfer," IEEE Microwave Magazine, 2015, **16**, (3), pp. 87-96.

[12] Collado, A., Georgiadis, A., "Improving wireless power transmission efficiency using chaotic waveforms," Proc. Int. Microw. Symp. (MTT-S),Montreal, Canada, 17-22 June 2012, pp. 1-3.

[13] Collado, A., Georgiadis, A., "Optimal Waveforms for Efficient Wireless Power Transmission," IEEE Microwave and Wireless Components Letters, 2014, **24**, (5), pp. 354-356.

[14] Fukuda G., Yoshida S., Kai Y., *et al.,* "Evaluation on use of modulated signal for Microwave Power Transmission," Proc. 44th European Microw. Conf. (EuMC), Rome, Italy, 6-9 Oct. 2014, pp. 425-428.

[15] Papoulis A. : 'Probability, Random Variables and Stochastic Processes, (McGraw Hill, 3rd Edn. 1991).

[16] Blanco, J., Bolos, F., Collado, A., et al., "RF-Energy Harvesting and Wireless Power Transfer Efficiency from Digitally Modulated Signals," Proc. Mediterranean Microwave Symposium (MMS), Lecce, Italy, 30 Nov- 2 Dec. 2015.